RESEARCH ARTICLE | DECEMBER 13 2024

Quasiperiodic shrimp-shaped domains in intrinsically coupled oscillators

Special Collection: From Sand to Shrimps: In Honor of Professor Jason A. C. Gallas

Silvio L. T. de Souza; Antonio M. Batista; Rene O. Medrano-T; Iberê L. Caldas

Chaos 34, 123146 (2024)
https://doi.org/10.1063/5.0234904

Chaos ARTICLE pubs.aip.org/aip/cha

Quasiperiodic shrimp-shaped domains in intrinsically coupled oscillators

Cite as: Chaos **34**, 123146 (2024); doi: 10.1063/5.0234904
Submitted: 23 August 2024 · Accepted: 25 November 2024 ·
Published Online: 13 December 2024

View Online Export Citation CrossMark

Silvio L. T. de Souza,[1,2,a)] Antonio M. Batista,[3,4] Rene O. Medrano-T,[5,6] and Iberê L. Caldas[2]

AFFILIATIONS

[1] Federal University of São João del-Rei, Campus Centro-Oeste, 35501-296 Divinópolis, MG, Brazil
[2] Institute of Physics, University of São Paulo, 05508-900 São Paulo, SP, Brazil
[3] Graduate Program in Science, State University of Ponta Grossa, 84030-900 Ponta Grossa, PR, Brazil
[4] Department of Mathematics and Statistics, State University of Ponta Grossa, 84030-900 Ponta Grossa, PR, Brazil
[5] Department of Physics, Federal University of São Paulo, UNIFESPF, Campus Diadema, 09913-030 Diadema, SP, Brazil
[6] Department of Physics, São Paulo State University, UNESP/IGCE, Campus Rio Claro, 13506-900 Rio Claro, SP, Brazil

Note: This paper is part of the Focus Issue, From Sand to Shrimps: In Honor of Professor Jason A. C. Gallas.
[a)] **Author to whom correspondence should be addressed:** thomaz@ufsj.edu.br

ABSTRACT

We report remarkable pattern formation of quasiperiodic domains in the two-dimensional parameter space of an intrinsically coupled system, comprising a rotor and a Duffing oscillator. In our analysis, we characterize the system using Lyapunov exponents, identifying self-similar islands composed of intricate regions of chaotic, quasiperiodic, and periodic behaviors. These islands form structures with an accumulation arrangement, denominated here as metamorphic tongues. Inside the islands, we observe Arnold tongues corresponding to periodic solutions. In addition, we surprisingly identify quasiperiodic shrimp-shaped domains that have been typically observed for periodic solutions. Similar features to the periodic case, such as period-doubling and secondary-near shrimp with three times the period, are observed in quasiperiodic shrimp as torus-doubling and torus-tripling.

In the context of nonlinear dynamics, several studies have reported the characterization of systems in the control parameter space. Periodic regimes are frequently observed, embedded in chaotic regions, presenting self-similar structures with highly organized patterns. Among the possible periodic structures, shrimp-shaped domains have been identified in a wide variety of dynamical systems, such as a predator–prey model, electrochemical oscillators, electronic circuits, and a two-gene model. More recently, shrimp-shaped domains associated with quasiperiodic regimes (torus attractors) were observed in a coupled radio-physical generator and in a discrete-time predator–prey model. In this work, we consider a mechanical oscillator with intrinsic coupling, focusing on the quasiperiodic scenario. As a key finding, we identify, in two-dimensional parameter space, quasiperiodic shrimp-shaped domains exhibiting interesting properties, such as self-similarity, highly organized pattern, torus-doubling, and torus-tripling regions.

I. INTRODUCTION

Over the past few decades, a considerable amount of work on nonlinear systems has examined the dynamics in two-dimensional parameter space using Lyapunov exponents.[1–4] Consequently, regular solutions have been visualized within continuous parameter planes, forming periodic structures embedded in quasiperiodic or chaotic regions. In numerous situations, the distribution of these periodic structures appears highly organized, exhibiting self-similarity and universal properties.[5–10] In this context, Arnold tongues and shrimp-shaped domains emerge prominently among the possible structures.[11–14] Shrimps, a term coined by Professor Jason Gallas,[11,12] have been identified for a dissipative model of relativistic particles,[15] a tumor growth model,[16] a predator–prey model,[17] electronic circuits,[18] a red grouse population model,[19] and plasma physics,[20] to name just a few. In the recent past, Stankevich and collaborators reported substantial findings on the study of quasiperiodicity, showing shrimp-shaped domains composed of quasiperiodic attractors.[21] More recently, Pati identified the existence of spiral connections for the self-organization of the quasiperiodic shrimps in a discrete-time predator–prey model.[22]

In nonlinear mechanics, intrinsically coupled oscillators represent an important class of systems with technological applications.[23–25] From a dynamical point of view, these oscillators have attracted significant attention due to their complexity, involving coexistence of attractors, quasiperiodicity, and chaotic vibrations.[26–28]

In this work, we investigate the parameter space organization of an intrinsically coupled system, composed of a rotor and a Duffing oscillator. Our main goal is to shed some light on the investigation of quasiperiodicity in two-dimensional parameter space.

This article is organized as follows: In Sec. II, we present the mathematical description of the rotor-Duffing oscillator using the Lagrangian formalism. In Sec. III, we show numerical findings from the characterization of quasiperiodic structures in two-dimensional parameter space. Section IV contains our main remarks.

II. ROTOR-DUFFING OSCILLATOR

In the context of the mathematical description for intrinsically coupled mechanical systems, Lagrangian formalism performs as a useful tool to determine the equations of motion.[29–31] We consider a coupled system combining a rotor and a Duffing oscillator. Figure 1 displays the schematic model of this coupled system, which includes a block with mass M connected to a fixed frame through a nonlinear spring, $-k_1X + k_2X^3$, and a dashpot, $b_1\dot{X}$. Mounted on the block is a rotor with mass m and length of the massless rod r. In this model, X represents the displacement of the block, while φ denotes the angular displacement of the rotor.

Using the Euler–Lagrange equations for kinetic energy and potential energy given by

$$T = \frac{m+M}{2}\dot{X}^2 + \frac{mr^2}{2}\dot{\varphi}^2 + mr\dot{X}\dot{\varphi}\cos(\varphi), \tag{1}$$

$$V = -\frac{k_1}{2}X^2 + \frac{k_2}{4}X^4, \tag{2}$$

adding the damping terms $b_1\dot{X}$ and $b_2\dot{\varphi}$, and including an excitation term, $E\cos(\omega_1 t)$, on the rotor, the equations of motion are given by

$$(m+M)\frac{d^2X}{dt^2} + b_1\frac{dX}{dt} - k_1X + k_2X^3 = mr\left(\frac{d\varphi}{dt}^2\sin\varphi - \frac{d^2\varphi}{dt^2}\cos\varphi\right), \tag{3}$$

$$mr^2\frac{d^2\varphi}{dt^2} + b_2\frac{d\varphi}{dt} = E\cos(\omega_1 t) - mr\frac{d^2X}{dt^2}\cos\varphi. \tag{4}$$

Considering $x \equiv X/r$ and derivatives with respect to τ, for $\tau \equiv \omega_0 t$ ($\omega_0 \equiv \sqrt{\frac{k_1}{m+M}}$), the equations of motion are reformulated as follows:

$$\ddot{x} + \beta_1\dot{x} - x + \gamma x^3 = \varepsilon\left(\dot{\varphi}^2\sin\varphi - \ddot{\varphi}\cos\varphi\right), \tag{5}$$

$$\ddot{\varphi} + \beta_2\dot{\varphi} = F\cos(\omega\tau) - \ddot{x}\cos\varphi \tag{6}$$

for $\beta_1 \equiv \frac{b_1}{(m+M)\omega_0}$, $\beta_2 \equiv \frac{b_2}{mr^2{\omega_0}^2}$, $\gamma \equiv \frac{k_2}{k_1}r^2$, $\varepsilon \equiv \frac{m}{m+M}$, $F \equiv \frac{E}{mr^2{\omega_0}^2}$, and $\omega \equiv \frac{\omega_1}{\omega_0}$.

These equations of motion align with a simplified mathematical model for non-ideal oscillators,[32–34] except for the periodic excitation term applied to the rotor.

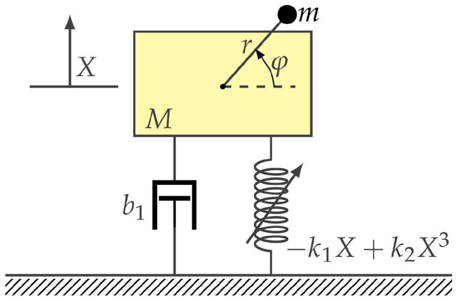

FIG. 1. Schematic model of the rotor-Duffing oscillator.

III. METAMORPHIC TONGUES AND QUASIPERIODIC SHRIMPS

In this section, we present a set of numerical results revealing a collection of remarkable dynamical domain organizations in two-parameter space for the rotor-Duffing oscillator. The simulations were performed by using the fourth-order Runge–Kutta method with a fixed time step of 10^{-2}. In addition, we discarded a transient phase of 2.0×10^5 iterations and utilized additional 2.0×10^7 trajectory points to compute the Lyapunov exponents. For our numerical analysis, we consider the control parameters F and ω from an excitation term, while the remaining control parameters were fixed at $\varepsilon = 0.025$, $\beta_1 = 0.02$, $\beta_2 = 1.5$, and $\gamma = 1.6$. The control parameter values correspond to those used in the numerical analysis to evaluate the experimental data from nonideal oscillators.[35]

Initially, to gain some insight into the dynamics, we investigate the system in terms of one-dimensional parameter ω for $F = 2.3$. Figures 2(a) and 2(b) display a bifurcation diagram and the corresponding Lyapunov exponent evaluation, respectively. For the bifurcation diagram, excluding the transient behavior of 2.0×10^5 iterations, we plot the asymptotic values of the local maxima x as a function of ω. We construct the diagram using the following attractor method. In other words, for each value of the parameter, we start the system by using the final state of the preceding parameter value as the initial conditions. In this case, we show only a transition sequence of attractors, omitting the multistability coexistences. To characterize the nature of the attractors, we evaluate the Lyapunov exponents using the Benettin algorithm,[36] with the code provided by Wolf and collaborators.[37] In Fig. 2(b), we plot three out of the five Lyapunov exponents, disregarding both the smallest and one of the

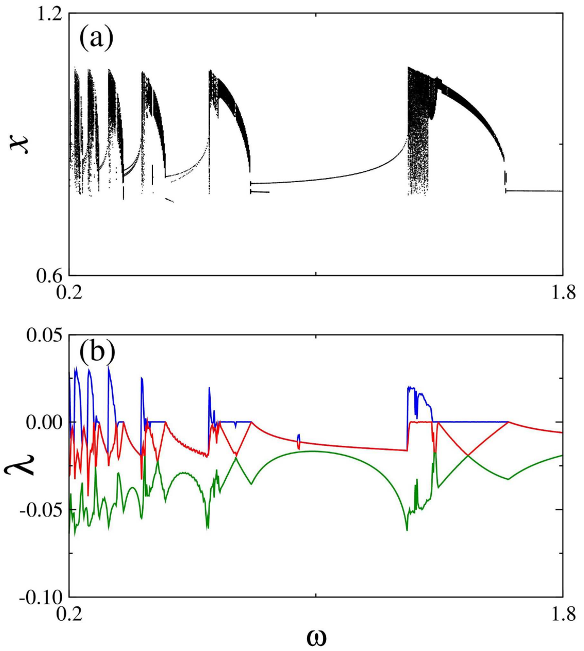

FIG. 2. (a) Bifurcation diagram for the local maxima of x as a function of ω with $F = 2.3$. (b) Three out of the five corresponding Lyapunov exponents, disregarding both the smallest and one of the null exponents. The remaining control parameters are fixed at $\varepsilon = 0.025$, $\beta_1 = 0.02$, $\beta_2 = 1.5$, and $\gamma = 1.6$.

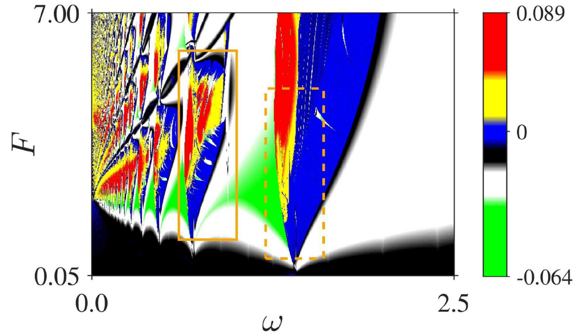

FIG. 3. Parameter plane diagram for F vs ω. Periodic solutions are plotted in white, black and green, quasiperiodic in blue, and chaotic in yellow and red. The remaining control parameters are fixed at $\varepsilon = 0.025$, $\beta_1 = 0.02$, $\beta_2 = 1.5$, and $\gamma = 1.6$.

null exponents. (To analyze a continuous-time system, we disconsider a zero exponent and focus on the largest Lyapunov exponent: positive indicates a chaotic attractor, negative indicates a periodic attractor, and zero indicates a quasiperiodic attractor.)

As a result of this preliminary numerical analysis, we learn that decreasing the control parameter results in an interesting pattern composed of an accumulating sequence of quasiperiodic and chaotic solutions, interspersed with periodic solutions.

To gain further insights, we should analyze the system using at least a two-dimensional parameter diagram. Along these lines, Fig. 3 exhibits a parameter plane diagram for F vs ω for a grid of 800×800 cells. The colors of the cells correspond to the range of the largest Lyapunov exponent values, excluding a null one, indicated in the bar on the right side of the figure. Periodic solutions are plotted in white, black, and green, quasiperiodic in blue, and chaotic in yellow and red. This parameter plane uncovers an outstanding pattern of formation behind the quasiperiodic–chaotic sequence of the bifurcation diagram shown in Fig. 2(a). Self-similar islands, surrounded by periodic regions, distribute along both parameters F and ω. Here, we observe the self-similar pattern even within the periodic domains. Green regions trace the compound islands spreading across the parameter plane, while black wave-like regions delineate the sequence of islands. Moreover, the narrow black strips between the white and blue regions indicate smooth transitions between periodic and quasiperiodic states. In this case, these compound islands predominantly blend both quasiperiodic and chaotic domains. In addition, the set of islands covers the parameter plane, forming metamorphic tongues, whose pattern of formation resembles the periodic resonance domains identified in parametric pendulums.[3]

To investigate the island structures in greater detail, we provide specific magnifications of the parameter plane. Figure 4(a) displays an overview of the region outlined by the golden solid-line box shown in Fig. 3. As mentioned before, the island is composed of different dynamical domains. Additionally, periodic structures arise in a recognizable way through the formation of resonance tongues, as shown in Fig. 4(b), 4cation of the golden dashed-line box in Fig. 4(a). These familiar structures, denominated Arnold tongues, are identified in a plethora of systems, from continuous-time mechanical oscillators[28] to discrete-time biological models.[38] In terms of the periodicity, these tongues exhibit both period-adding and Fibonacci-type sequences.[5]

Shifting our focus to quasiperiodic domains, we present in Fig. 4(c) a magnification of the golden dashed-line box shown in Fig. 3 and in Figs. 4(d)–4(f) successive magnifications of Fig. 4(c). Surprisingly, the quasiperiodicity, in blue, appears well structured, manifesting as shrimp-shaped forms, and highly organized for some portions of the parameter plane, as evidenced in Figs. 4(e) and 4(f).

Shedding some light on quasiperiodic shrimp-shaped domains, we reevaluate the parameter plane by focusing on the third largest Lyapunov exponent. In quasiperiodic domains, valuable information lies in the third largest exponent, such as torus bifurcation lines where this exponent is zero. For regions involving only quasiperiodic and chaotic attractors with two zero Lyapunov exponents, we can easily characterize the parameter plane by summing the three largest Lyapunov exponents. Figure 5(a) shows, with this new approach, the same portion of the parameter plane depicted in Fig. 4(e). Chaotic regions are plotted in white, quasiperiodic domains in black and green, and the torus-doubling bifurcations, with three zero exponents, are highlighted in blue. In this case, as observed for the coupled radio-physical generators,[21] the quasiperiodic shrimps are surrounded by chaos with two zero Lyapunov exponents. In Fig. 5(b), we provide a magnification of the rectangular area (golden box) from Fig. 5(a), revealing, similar to the periodic shrimps, a highly organized sequence of secondary shrimps near the

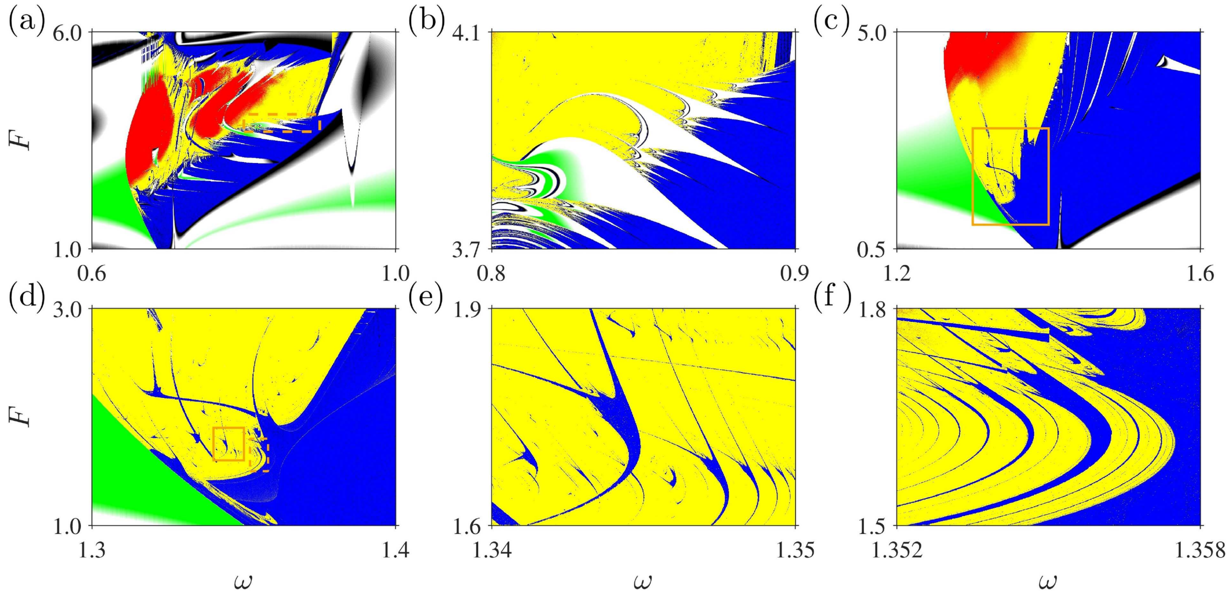

FIG. 4. Parameter plane diagrams showing magnified views of selected regions: (a) the solid-line box from Fig. 3, (b) the dashed-line box from Fig. 4(a), (c) the dashed-line box from Fig. 3, (d) the solid-line box from Fig. 4(c), (e) the solid-line box from Fig. 4(d), and (f) the dashed-line box from 4(d).

legs of the main shrimp. In the periodic case, the shrimps satisfy the three times self-similar property.[5,6] In other words, the largest secondary shrimps exhibit a period that is three times the period of the corresponding main shrimps.

For the cross section of the shrimp domain shown with a dashed line in Fig. 5(a), Figs. 6(a) and 6(b) display for $F = 1.72$ a bifurcation diagram of ω and three out of five corresponding Lyapunov exponents, respectively. The smallest and trivial zero exponents associated with time are not plotted. Chaotic range, besides a positive exponent in blue, are distinguished by two zero exponents: one in red and another not plotted. In the quasiperiodic case indicating torus-doubling bifurcations, some points exhibit three zero exponents: two in blue and red and one not plotted.

Figures 7(a)–7(d) display a complete overview of the torus attractors belonging to the quasiperiodic shrimp-shaped domains. Using stroboscopic mapping to collect the data, obtaining points periodically for $T = 2\pi n/\omega$, Fig. 7(a) shows for $F = 1.72$ and $\omega = 1.3446$ a torus, in blue, and in the background, for $F = 1.72$ and $\omega = 1.3435$ a chaos-torus in gray. These attractors correspond to the dashed lines depicted in the bifurcation diagram of Fig. 6(a). Figure 7(b) illustrates a torus-doubling case for $F = 1.776$ and $\omega = 1.343\,64$, marked with a yellow X symbol in the shrimp of Fig. 5(b). Figure 7(c) displays a torus-tripling case for $F = 1.784$ and $\omega = 1.343\,35$, indicated with a yellow cross in the largest secondary shrimp of Fig. 5(b). In the end, from a magnification of a small part of these tori in Fig. 7(d), we highlight the torus-doubling and torus-tripling phenomena, comparing a single torus in blue to a double torus in red and a triple torus in green.

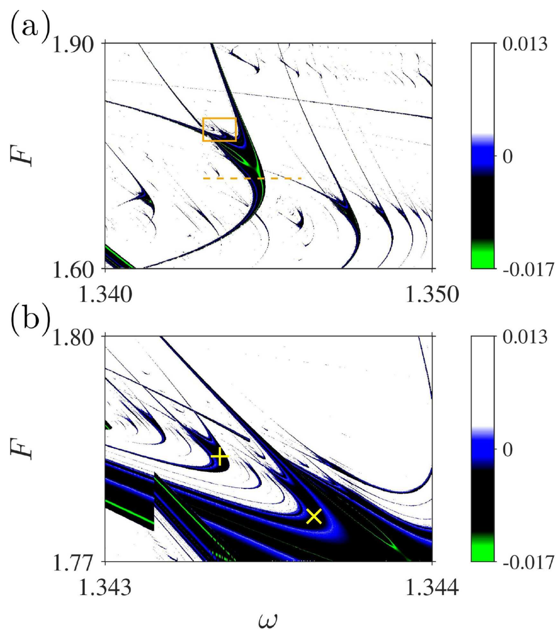

FIG. 5. (a) Diagram for the sum of the three largest Lyapunov exponents for the same portion of the parameter plane as in Fig. 4(e). (b) A magnified view of the box from Fig. 5(a). Chaotic regions are plotted in white, quasiperiodic domains in black and green, and torus-doubling bifurcations, with three zero Lyapunov exponents, in blue.

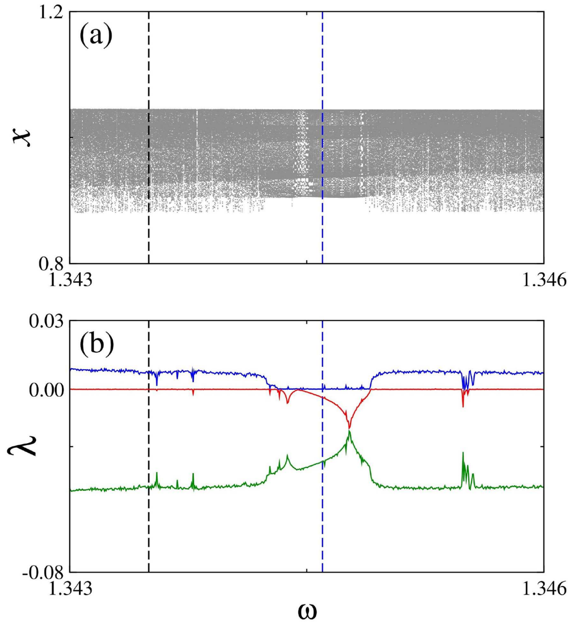

FIG. 6. (a) Bifurcation diagram for $F = 1.72$ following the cross-sectional dashed line of the shrimp from Fig. 5 (a). (b) Three out of the five corresponding Lyapunov exponents.

IV. FINAL REMARKS

In this study, we characterized the dynamics of a rotor-Duffing oscillator in two-dimensional parameter space, considering the parameters of the excitation function. By using Lyapunov exponent evaluations, we identified a set of self-similar islands exhibiting an interwoven pattern of chaotic, quasiperiodic, and periodic regions. These islands present a distinguished accumulation arrangement, termed here as metamorphic tongues. Moreover, we observed Arnold tongues as periodic structures, forming boundaries between quasiperiodic and chaotic regions for certain parts of the islands.

Most remarkably, we identified quasiperiodic shrimp-shaped domains, a type of structure typically associated with periodic solutions. These quasiperiodic shrimps exhibit interesting properties, such as torus-doubling and torus-tripling, corresponding, in the periodic case, to period-doubling and period-three-times attractors, respectively.

To conclude, the findings expand our understanding of nonlinear dynamical behaviors for coupled systems, highlighting the importance of quasiperiodic solutions due to intrinsically coupling interactions.

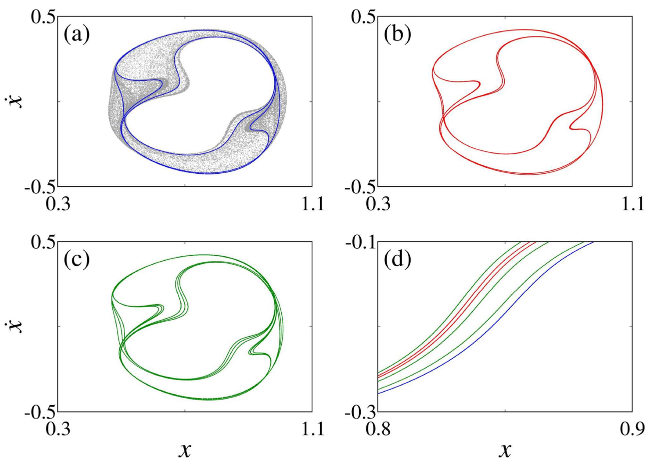

FIG. 7. Overview of the attractors: (a) Torus in blue for (ω, F) = (1.3446, 1.72) and chaos-torus in gray for (ω, F) = (1.3435, 1.72). These attractors are indicated by dashed lines in the bifurcation diagram from Fig. 6(a). (b) Torus-doubling for (ω, F) = (1.343 64, 1.776), indicated with a yellow x in Fig. 5(b). (c) Torus-tripling for (ω, F) = (1.343 35, 1.784), indicated with a yellow cross in Fig. 5(b). (d) Magnified comparison of the attractors showing the doubling, in red, and tripling, in green, of the torus, in blue.

ACKNOWLEDGMENTS

This study was supported by the São Paulo Research Foundation (FAPESP) under Grant Nos. 2018/03211-6, 2024/05176-4, 2024/14478-4, and 2024/06718-5. We are grateful for their financial support, which made this research possible. We acknowledge the 105 Group Science members for their insightful discussions (https://www.105groupscience.com).

AUTHOR DECLARATIONS

Conflict of Interest

The authors have no conflicts to disclose.

Author Contributions

Silvio L. T. de Souza: Conceptualization (equal); Data curation (equal); Formal analysis (equal); Investigation (equal); Methodology (equal); Writing – original draft (equal); Writing – review & editing (equal). **Antonio M. Batista:** Conceptualization (equal); Data curation (equal); Formal analysis (equal); Validation (equal); Writing – original draft (equal); Writing – review & editing (equal). **Rene O. Medrano-T:** Conceptualization (equal); Validation (equal); Writing – review & editing (equal). **Iberê L. Caldas:** Conceptualization (equal); Formal analysis (equal); Funding acquisition (lead); Methodology (equal); Writing – original draft (equal); Writing – review & editing (equal).

DATA AVAILABILITY

The data that support the findings of this study are available from the corresponding author upon reasonable request.

REFERENCES

[1]E. Barreto, B. R. Hunt, C. Grebogi, and J. A. Yorke, "From high dimensional chaos to stable periodic orbits: The structure of parameter space," Phys. Rev. Lett. **78**, 4561–4564 (1997).
[2]S. L. T. de Souza and I. L. Caldas, "Calculation of Lyapunov exponents in systems with impacts," Chaos, Solitons Fractals **19**, 569–579 (2004).

[3] X. Xu, M. Wiercigroch, and M. P. Cartmell, "Rotating orbits of a parametrically-excited pendulum," Chaos, Solitons Fractals **23**, 1537–1548 (2005).
[4] F. Hegedüs, W. Lauterborn, U. Parlitz, and R. Mettin, "Non-feedback technique to directly control multistability in nonlinear oscillators by dual-frequency driving: GPU accelerated topological analysis of a bubble in water," Nonlinear Dyn. **94**, 273–293 (2018).
[5] S. L. T. de Souza, A. A. Lima, I. L. Caldas, R. O. Medrano-T., and Z. O. Guimarães-Filho, "Self-similarities of periodic structures for a discrete model of a two-gene system," Phys. Lett. A **376**, 1290–1294 (2012).
[6] R. Kumbhakar, M. Hossain, S. Karmakar, and N. Pal, "An investigation of the parameter space in a tri-trophic food chain model with refuge," Math. Comput. Simul. **217**, 37–59 (2024).
[7] E. S. Medeiros, R. O. Medrano-T, I. L. Caldas, and S. L. T. de Souza, "Torsion-adding and asymptotic winding number for periodic window sequences," Phys. Lett. A **377**, 628–631 (2013).
[8] M. J. B. Hauser and J. A. C. Gallas, "Nonchaos-mediated mixed-mode oscillations in an enzyme reaction system," J. Phys. Chem. Lett. **5**, 4187–4193 (2014).
[9] D. R. da Costa, M. Hansen, G. Guarise, R. O. Medrano-T, and E. D. Leonel, "The role of extreme orbits in the global organization of periodic regions in parameter space for one dimensional maps," Phys. Lett. A **380**, 1610–1614 (2016).
[10] R. Varga, K. Klapcsik, and F. Hegedüs, "Route to shrimps: Dissipation driven formation of shrimp-shaped domains," Chaos, Solitons Fractals **130**, 109424 (2020).
[11] J. A. C. Gallas, "Structure of the parameter space of the Hénon map," Phys. Rev. Lett. **70**, 2714–2717 (1993).
[12] J. A. Gallas, "Dissecting shrimps: Results for some one-dimensional physical models," Physica A **202**, 196–223 (1994).
[13] M. S. Baptista and I. L. Caldas, "Dynamics of the kicked logistic map," Chaos, Solitons Fractals **7**, 325–336 (1996).
[14] A. Celestino, C. Manchein, H. A. Albuquerque, and M. W. Beims, "Ratchet transport and periodic structures in parameter space," Phys. Rev. Lett. **106**, 234101 (2011).
[15] M. Hansen, D. R. da Costa, D. F. M. Oliveira, and E. D. Leonel, "Statistical properties for a dissipative model of relativistic particles in a wave packet: A parameter space investigation," Appl. Math. Comput. **238**, 387–392 (2014).
[16] C. Stegemann and P. C. Rech, "Organization of the dynamics in a parameter plane of a tumor growth mathematical model," Int. J. Bifurcation Chaos **24**, 1450023 (2014).
[17] M. Hossain, S. Garai, S. Jafari, and N. Pal, "Bifurcation, chaos, multistability, and organized structures in a predator–prey model with vigilance," Chaos **32**, 063139 (2022).
[18] H. A. Albuquerque, R. M. Rubinger, and P. C. Rech, "Self-similar structures in a 2D parameter-space of an inductorless Chua's circuit," Phys. Lett. A **372**, 4793–4798 (2008).
[19] J. Slipantschuk, E. Ullner, M. S. Baptista, M. Zeineddine, and M. Thiel, "Abundance of stable periodic behavior in a red grouse population model with delay: A consequence of homoclinicity," Chaos **20**, 045117 (2010).
[20] A. A. Alvarez, E. L. Brugnago, and I. L. Caldas, "Routes to chaos and bistability in the Rypdal model with a parametric disturbance," Chaos, Solitons Fractals **186**, 115246 (2024).
[21] N. V. Stankevich, N. A. Shchegoleva, I. R. Sataev, and A. P. Kuznetsov, "Three-dimensional torus breakdown and chaos with two zero Lyapunov exponents in coupled radio-physical generators," J. Comput. Nonlinear Dyn. **15**, 111001 (2020).
[22] N. C. Pati, "Spiral organization of quasi-periodic shrimp-shaped domains in a discrete predator–prey system," Chaos **34**, 083126 (2024).
[23] D. Wang, F. Chen, Z. Hao, and M. Wiercigroch, "Nonlinear energy harvesting from rotating system," Commun. Nonlinear Sci. Numer. Simul. **127**, 107521 (2023).
[24] S.-H. Teh, K.-C. Woo, and M. Wiercigroch, "Nonlinear dynamics of vibro-impacting indenter," Appl. Sci. **13**, 2469 (2023).
[25] L. G. Costa and M. A. Savi, "Pendulum-based hybrid system for multidirectional energy harvesting," Nonlinear Dyn. **112**, 18665–18684 (2024).
[26] B. R. Nana Nbendjo, I. L. Caldas, and R. L. Viana, "Dynamical changes from harmonic vibrations of a limited power supply driving a Duffing oscillator," Nonlinear Dyn. **70**, 401–407 (2012).
[27] A. S. de Paula, M. A. Savi, M. Wiercigroch, and E. Pavlovskaia, "Bifurcation control of a parametric pendulum," Int. J. Bifurcation Chaos **22**, 1250111 (2012).
[28] S. L. T. de Souza, A. M. Batista, M. S. Baptista, I. L. Caldas, and J. M. Balthazar, "Characterization in bi-parameter space of a non-ideal oscillator," Physica A **466**, 224–231 (2017).
[29] J. Warminski and K. Kecik, "Instabilities in the main parametric resonance area of a mechanical system with a pendulum," J. Sound Vibr. **322**, 612–628 (2009).
[30] P. Brzeski, P. Perlikowski, S. Yanchuk, and T. Kapitaniak, "The dynamics of the pendulum suspended on the forced Duffing oscillator," J. Sound Vibr. **331**, 5347–5357 (2012).
[31] M. Kapitaniak, P. Perlikowski, and T. Kapitaniak, "Synchronous motion of two vertically excited planar elastic pendula," Commun. Nonlinear Sci. Numer. Simul. **18**, 2088–2096 (2013).
[32] S. L. T. de Souza, I. L. Caldas, R. L. Viana, J. M. Balthazar, and R. M. L. R. F. Brasil, "Impact dampers for controlling chaos in systems with limited power supply," J. Sound Vibr. **279**, 955–967 (2005).
[33] V. Piccirillo, J. M. Balthazar, B. R. Pontes, and J. L. P. Felix, "Chaos control of a nonlinear oscillator with shape memory alloy using an optimal linear control: Part II: Nonideal energy source," Nonlinear Dyn. **56**, 243–253 (2009).
[34] J. M. Balthazar, A. M. Tusset, R. M. L. R. F. Brasil, J. L. P. Felix, R. T. Rocha, F. C. Janzen, A. Nabarrete, and C. Oliveira, "An overview on the appearance of the Sommerfeld effect and saturation phenomenon in non-ideal vibrating systems (NIS) in macro and MEMS scales," Nonlinear Dyn. **93**, 19–40 (2018).
[35] P. Gonçalves, M. Silveira, B. Pontes Junior, and J. Balthazar, "The dynamic behavior of a cantilever beam coupled to a non-ideal unbalanced motor through numerical and experimental analysis," J. Sound Vibr. **333**, 5115–5129 (2014).
[36] G. Benettin, L. Galgani, A. Giorgilli, and J.-M. Strelcyn, "Lyapunov characteristic exponents for smooth dynamical systems and for Hamiltonian systems; a method for computing all of them. Part 1: Theory," Meccanica **15**, 9–20 (1980).
[37] A. Wolf, J. B. Swift, H. L. Swinney, and J. A. Vastano, "Determining Lyapunov exponents from a time series," Physica D **16**, 285–317 (1985).
[38] S. Garai, M. Hossain, S. Karmakar, and N. Pal, "Chaos, periodic structures, and multistability: Complex dynamical behaviors of an eco-epidemiological model in parameter planes," Chaos **33**, 083115 (2023).